J Mol Model (2013) 19:757–765
DOI 10.1007/s00894-012-1598-6

ORIGINAL PAPER

Modeling the effect of H-bonding interactions and molecular packing on the molecular structure of $[Ag(ethylnicotinate)_2]NO_3$ complex

Saied M. Soliman

Received: 20 June 2012 / Accepted: 19 September 2012 / Published online: 9 October 2012

Abstract The gas phase molecular structure of a single isolated molecule of $[Ag(Etnic)_2NO_3]$;**1** where Etnic = Ethylnicotinate was calculated using B3LYP method. The H-bonding interaction between **1** with one (complex **2**) and two (complex **3**) water molecules together with the dimeric formula $[Ag(Etnic)_2NO_3]_2$;**4** and the tetrameric formula $[Ag(Etnic)_2NO_3]_4$;**5** were calculated using the same level of theory to model the effect of intermolecular interactions and molecular packing on the molecular structure of the titled complex. The H-bond dissociation energies of complexes **2** and **3** were calculated to be in the range of 12.220–14.253 and 30.106–31.055 kcalmol^{-1}, respectively, indicating the formation of relatively strong H-bonds between **1** and water molecules. The calculations predict bidentate nitrate ligand in the case of **1** and **2**, leading to distorted tetrahedral geometry around the silver ion with longer Ag–O distances in case of **2** compared to **1**, while **3** has a unidentate nitrate ligand leading to a distorted trigonal planar geometry. The packing of two $[Ag(Etnic)_2NO_3]$ complex units; **4** does not affect the molecular geometry around Ag(I) ion compared to **1**. In the case of **5**, the two asymmetric units of the formula $[Ag(Etnic)_2NO_3]$ differ in the bonding mode of the nitrate group, where the geometry around the silver ion is distorted tetrahedral in one unit and trigonal planar in the other. The calculations predicted almost no change in the charge densities at the different atomic sites except at the sites involved in the C–H···O interactions as well as at the coordinated nitrogen of the pyridine ring.

Keywords H-bonding · Packing · Silver · Ethylnicotinate · DFT

Introduction

Intermolecular interactions such as hydrogen bonds between molecules have attracted the attention of many researchers [1–4]. Hydrogen bonding is considered the principal mode of noncovalent interaction, not only affecting the activities of many biological molecules but also playing an important role in stabilizing and determining their structure and shape [5].

In recent years, silver compounds have attracted much attention due to their antimicrobial activity; silver ions do not show toxicity and carcinogenic activities in the range of concentrations applied [6–9]. As a result, there is increased interest in discovering more potential uses of silver(I) as a therapeutic agent for different antimicrobial applications [10–16]. Silver (I) complexes of the formula AgL_2NO_3, where L is a monodentate N-donor ligand, possess different molecular geometry and supramolecular structures depending on the nature of the ligand (L) and the bonding mode of the nitrate group. Recently, our research group has focused on the synthesis and molecular structure of different silver (I) nitrate complexes with quinoxaline and pyridine derivatives [17–22]. It was found that the nitrate ion may be free, or act as a monodentate or bidentate ligand through the oxygen atoms, which leads to different coordination geometries around the silver ion such as linear, bent, trigonal planar or tetrahedral [22–27]. The factors affecting the molecular geometry of such complexes are still not well elucidated.

Since quantum chemical calculations have proved to offer excellent prediction in determining the molecular

Electronic supplementary material The online version of this article (doi:10.1007/s00894-012-1598-6) contains supplementary material, which is available to authorized users.

S. M. Soliman (✉)
Department of Chemistry, Faculty of Science,
Alexandria University,
PO Box 426, Ibrahimia,
21525 Alexandria, Egypt
e-mail: Saied1soliman@yahoo.com

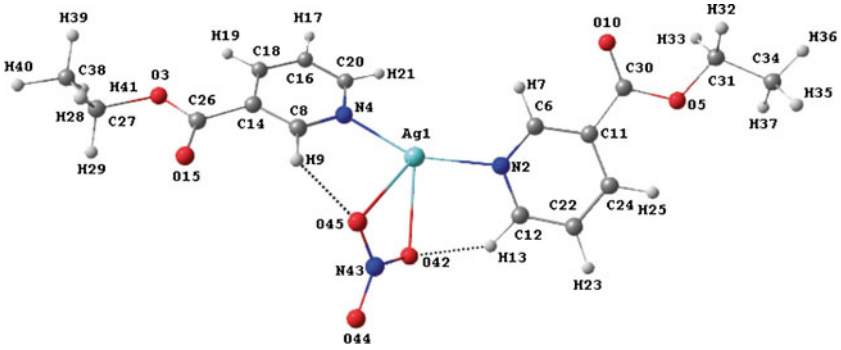

Fig. 1 Calculated optimized molecular geometry of a single molecule of $[Ag(Etnic)_2]NO_3$; **1** using B3LYP/LANL2DZ

structure of a variety of organic and inorganic systems [25–40] as well as being useful for studying the intermolecular interactions between two or more H-bonded molecules, the present work aims to calculate the gas phase molecular geometry of a single isolated $[Ag(Etnic)_2]NO_3$ molecule using DFT/B3LYP method. The results were compared with X-ray structure data available from the Cambridge Crystallographic Data Center (CCDC) [41], and the interaction between $[Ag(Etnic)_2]NO_3$ with one and two water molecules was calculated to model the effect of the H-bonding interaction on the molecular structure of the titled complex. Dimeric and tetrameric formula of the $[Ag(Etnic)_2]NO_3$ complex were also calculated using the same level of theory in order to simulate the effect of molecular packing on the molecular structure of the studied silver complex.

Theoretical considerations

All calculations for the $[Ag(Etnic)_2]NO_3$ complex, its H-bonded complexes with one $Ag(Etnic)_2NO_3\cdots H_2O$; **2** and two water molecules $Ag(Etnic)_2NO_3\cdots 2H_2O$; **3** as well as the dimer $[Ag(Etnic)_2NO_3]_2$; **4** and tetramer $[Ag(Etnic)_2NO_3]_4$; **5** were carried out using Gaussian 03 software [42]. All complexes were calculated using B3LYP/LANL2DZ method. Also, all complexes except **5** were calculated using the same theory but using the 6–31G(d, p) basis set for all atoms except for silver, where the ECP/LANL08 basis set was used [43]. Furthermore, complexes **2** and **3** were calculated using MPWPW91 and PEB1PBE DFT methods, which were found to be more specific for investigating the H-bonding interactions [44]. The input structure of the studied silver complex was

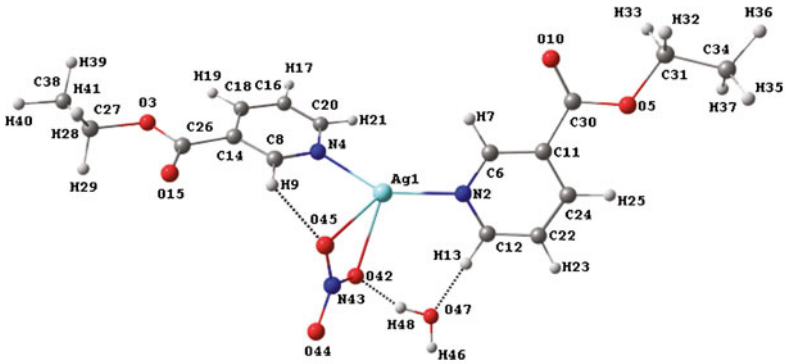

Complex 2

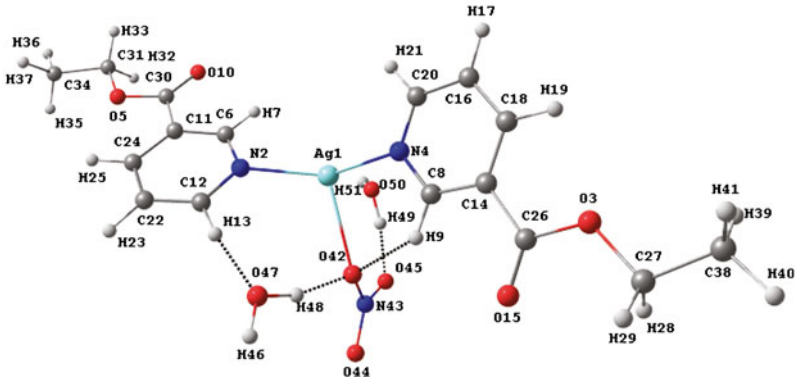

Complex 3

taken from the crystallographic information file (CIF) obtained from CCDC [41]. Gauss view [45] was used to draw the structures of the optimized geometries. The starting input of complexes **1**, **4** and **5** were taken from the CIF of the [Ag $(Etnic)_2]NO_3$ complex obtained from the CCDC. In the case of complexes **2** and **3**, the water molecules were placed close as possible to the nitrate ion, and situated appropriately for H-bonding with its O-atoms.

Results and discussion

Stabilities, dipole moments and thermodynamic functions

The optimized structures of complexes (**1–5**) are shown in Figs. 1, 2 and 3. Selected comparative DFT calculated bond distances and bond angles are given in Table 1. The calculated total energies and dipole moments of the studied complexes together with the H-bond dissociation energies of complexes **2** and **3** are given in Table 2. Generally, the interaction energies (ΔE) between two molecules A and B are calculated as the energy difference between the product complex $E_{(AB)}$ and its components $E_{(A)}$ and $E_{(B)}$.

$$\Delta E = E_{(AB)} - E_{(A)} - E_{(B)} \quad (1)$$

The H-bond dissociation energies of complexes **2** and **3** using DFT/B3LYP method were calculated to be 13.757 and 30.106 kcalmol^{-1}, respectively. MPWPW91 and PEB1PBE functions were reported [44] to give better performance for studying hydrogen bonding interactions than the B3LYP method. As a result, the H-bonding interactions of complex **1** with one and two water molecules were calculated using these methods; the results of interaction energies are given in Table 2. It can be seen that these functions overestimate the calculated H-bond dissociation energies (ΔE) compared to the conventional B3LYP method. Furthermore, the mp2 interaction energies, including BSSE correction at the B3LYP optimized structure of these complexes, were calculated using the Counterpoise method. The more accurate H-bond dissociation energies of complexes **2** and **3** were calculated to be −12.22 and −30.78 kcalmol^{-1}, respectively. These results indicate relatively

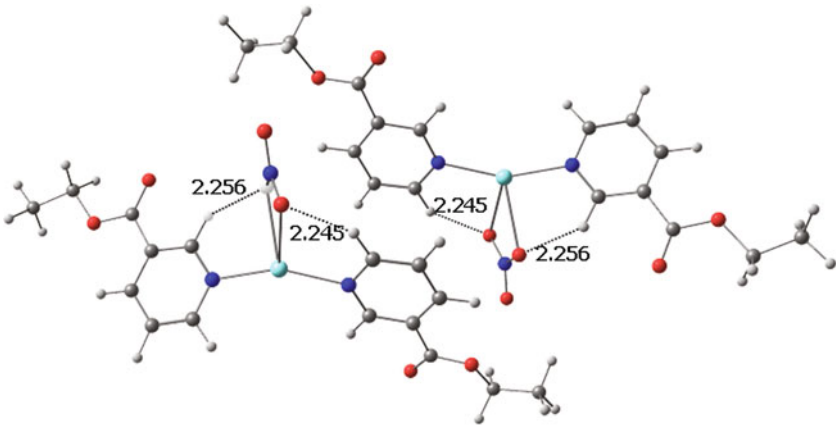

Complex 4

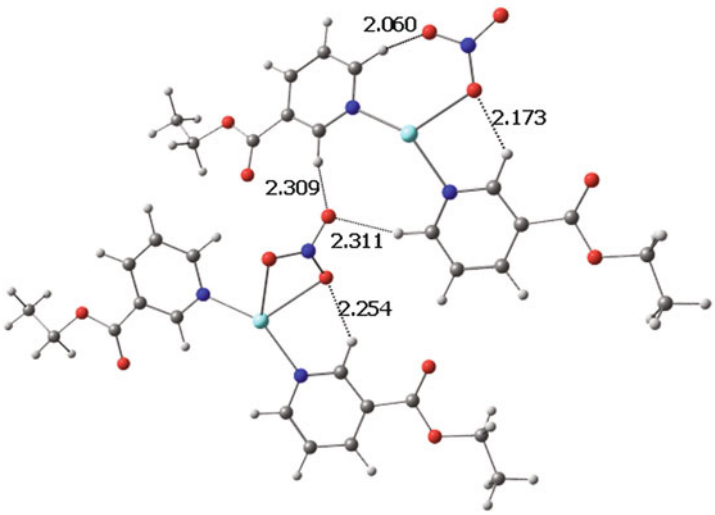

Complex 5

Fig. 3 Calculated optimized molecular geometry of the dimer $[Ag(Etnic)_2NO_3]_2$, **4** and one asymmetric unit of the tetramer $[Ag(Etnic)_2NO_3]_4$, **5** using the B3LYP/LANL2DZ method

Table 1 Selected calculated geometric parameters [bond distances (Å) and bond angles (°)] for the studied complexes

Parameter	B3LYP/6-31Gd,p/LANL08				B3LYP/LANL2DZ					MPWPW91/LANL2DZ			PEB1PBE/LANL2DZ			Experimental [19]
	1	**2**	**3**	**4**	**1**	**2**	**3**	**4**	**5**	**1**	**2**	**3**	**1**	**2**	**3**	
Ag1-N2	2.283	2.252	2.258	2.254	2.248	2.241	2.262	2.221	2.211	2.204	2.185	2.203	2.222	2.213	2.23449	2.146
Ag1-N4	2.280	2.263	2.313	2.270	2.250	2.27	2.293	2.236	2.250	2.205	2.209	2.221	2.224	2.241	2.260	2.152
Ag1-O42	2.472	2.518	2.478	2.491	2.545	2.505	2.590	2.589	2.683	2.573	2.538	2.601	2.557	2.493	2.57248	2.987
Ag1-O45	2.482	2.543	3.503	2.547	2.576	2.638	3.748	2.625	2.637	2.555	2.679	3.761	2.526	2.617	3.73237	4.510
O42□H13	2.199	-	-	2.337	2.109	-	-	2.245	-	2.115	-	-	2.081	-	-	2.393
O45□H9	2.309	2.322	-	2.320	2.217	2.279	-	2.256	2.254	2.231	2.284	-	2.189	2.254	-	2.660
O42□H48	-	1.947	1.889	-	-	1.684	1.700	-	-	-	1.662	1.687	-	1.661	1.67643	-
O45□H49	-	-	1.728	-	-	-	1.647	-	-	-	-	1.623	-	-	1.63254	-
O47□H13	-	2.230	2.072	-	-	1.945	1.942	-	-	-	1.927	1.920	-	1.912	1.91602	-
N2-Ag1-N4	152.573	156.586	151.246	153.530	153.886	147.637	142.227	156.639	148.530	156.251	155.531	152.380	154.046	148.680	144.143	175.353
O42-Ag1-O45	52.573	51.282	-	51.571	52.538	52.078	-	51.552	50.329	53.166	51.927	-	52.406	51.898	-	-
N2-Ag1- O42	89.805	94.798	109.177	90.358	87.152	107.306	109.731	88.048	89.907	88.271	106.470	106.272	87.170	107.820	109.670	-
N2-Ag1- O45	113.84	109.463	-	113.107	116.583	119.597	-	113.082	124.021	112.823	111.226	-	116.415	118.640	-	-
N4-Ag1- O42	115.17	106.974	86.302	112.368	116.397	103.172	88.203	111.916	118.401	113.015	96.443	88.869	116.249	101.571	88.178	-
N4-Ag1- O45	91.375	91.236	-	92.498	88.092	87.845	-	89.858	86.623	89.243	89.530	-	88.104	88.018	-	-
N43–O42□H48	-	103.403	106.193	-	-	122.746	119.508	-	-	-	115.404	113.169	-	122.484	119.560	-
N43–O45□H49	-	-	113.787	-	-	-	115.244	-	-	-	-	114.107	-	-	114.832	-
C12–H13□O47	-	153.871	175.390	-	-	176.193	168.353	-	-	-	174.736	167.727	-	176.062	166.555	-

Table 2 Calculated energies (E_{Tot}), interaction energies (ΔE), dipole moments (μ) and thermodynamic functions for the studied complexes using different methods at LANL2DZ basis set

Complex	−ΔE (kcal/mol)				μ[a] (Debye)	C_v [a] cal/molK	S [a] (cal/molK)
	B3LYP	MPWPW91	PEB1PBE	mp2			
1	-	-	-	-	10.953	99.080	207.615
2	13.757	13.848	14.253	12.220	9.914	108.624	226.112
3	30.106	30.248	31.055	30.779	9.641	117.548	240.090
4	15.883	-	-	-	0.000	-	-
5	62.454	-	-	-	0.000	-	-

[a] B3LYP/LANL2DZ

moderate-to-strong H-bonding interactions between complex **1** and water molecules. The calculated dipole moments of complexes **1**–**3** are calculated to be 10.953, 9.9139 and 9.6412 Debye, respectively. These results indicate a decrease in molecule polarity due to the H-bonding interactions with water molecules. On other hand, the optimized molecular geometry of complexes **4** and **5** possesses a C_i point group so the calculated dipole moments for these complexes are equal to zero Debye due to symmetry considerations. The calculated constant volume molar heat capacity (C_v) and entropy (S) of complexes **1**–**3** are given in Table 2. It can be noted that the interaction of water molecules with the $[Ag(Etnic)_2]NO_3$ increases not only the absolute entropy of the system but also its molar heat capacity at constant volume (C_v) due to the increased number of degrees of freedom of the system.

Structure description

The calculated optimized molecular geometry of the studied complexes **1**–**5** at the DFT/B3LYP level of theory are given in the Supplementary data. In the present work, the effect of H-bonding interactions on the coordination geometry around the silver ion was studied by comparing geometric parameters such as bond distances and bond angles around metal ion for complexes **1–5** with the X-ray solid state structure of **1** [19].

Molecular structure of $[Ag(Etnic)_2NO_3]$, **1**

The gaseous phase molecular geometry of a single isolated molecule of the titled complex calculated using the B3LYP/LANL2DZ method is shown in Fig. 1. It can be seen from Table 1 that the calculated Ag–N(py) and Ag–O distances are in the range of 2.248–2.283 Å and 2.472–2.576 Å, respectively, indicating distorted tetrahedral geometry around the silver ion where the nitrate group acts as a bidentate ligand through two O-atoms. The X-ray single crystal structure of this complex showed that the shortest Ag–O distance is 2.825 Å, indicating uncoordinated nitrate and almost a linear geometry around the silver ion [19]. These results indicate that the electrostatic interaction between the Ag^+ ion and the nitrate group is the dominant processes in the gas phase where there are no intermolecular interactions to be considered. Also, calculations predicted the O42···H13 and O45···H9 distances to be in the range of 2.109–2.199 Å and 2.279–2.309 Å, respectively, which indicates the presence of intramolecular C-H···O interactions between the O-atoms of the nitrate group and neighboring H-atoms [22].

Molecular structure of $Ag(Etnic)_2NO_3\cdots nH_2O$, **2** *and* **3**

In order to model the effect of the H-bonding interactions on the bonding mode of the nitrate group as well as on the molecular geometry around the Ag^+ ion, the interaction of complex **1** with one and two water molecules was calculated at the same level of theory. The optimized molecular geometries of $Ag(Etnic)_2NO_3\cdots H_2O$; **2** and $Ag(Etnic)_2NO_3\cdots 2H_2O$; **3** are shown in Fig. 2 and the results of the most significant geometric parameters as well as the H-bonding information are given in Table 1.

The H-bonding interaction between the nitrate group and one water molecule almost does not affect the coordination geometry around the metal ion. Although the calculated Ag–O distances are increased slightly up to 2.638 Å, they are still less than the summation of the Van der Waals radii of the two elements, indicating that the bonding situation of the nitrate group is almost unchanged compared to $[Ag(Etnic)_2NO_3]$. On the other hand, the interaction with another water molecule changes the geometry around the silver ion from distorted tetrahedral to distorted trigonal planar geometry where one Ag–O distance is calculated in the range of 2.478–2.590 Å while the other is in the range of 3.503–3.748 Å. The latter is too long, indicating that the nitrate ion acts as a unidentate ligand through one oxygen atom. Also, the intramolecular C–H···O interactions become much weaker and are less significant than the intermolecular C–H···O interactions formed between the water molecules and the adjacent hydrogen atoms of the pyridine ring (see Fig. 2 and Table 1). Anyway, the presence of these H-bonding interactions tends to weaken the Ag–O(NO_2) interactions.

Molecular structure of $[Ag(Etnic)_2NO_3]_n$, **4** *and* **5**

In order to model the effect of molecular packing on the molecular geometry of the studied silver complex, the dimer $[Ag(Etnic)_2NO_3]_2$; **4** and tetramer $[Ag(Etnic)_2NO_3]_4$; **5** were

Table 3 Calculated Mülliken atomic charge (MAC) densities for the studied complexes using DFT/B3LYP/LANL2DZ

	Etnic	**1**	**2**	**3**	**4**	**5**	
Ag1	-	0.3858	0.395	0.3961	0.3831	0.3948	0.3902
N2	-0.0139[a]	-0.2016[a]	-0.2171[a]	-0.207[a]	-0.2198[a]	-0.235[a]8	-0.2237[a]
O3	-0.3333	-0.3374	-0.3365	-0.3355	-0.3353	-0.3295	-0.3385
N4	-0.0139[a]	-0.2019[a]	-0.1935[a]	-0.1802[a]	-0.2073[a]	-0.2038[a]	-0.2122[a]
O5	-0.3333	-0.3291	-0.3294	-0.3295	-0.3161	-0.3254	-0.3332
C6	-0.402[a]	-0.3025[a]	-0.2737[a]	-0.2899[a]	-0.3057[a]	-0.2958[a]	-0.294[a]
H7	0.2784	0.2823	0.2795	0.2782	0.2794	0.27	0.3209
C8	-0.402[a]	-0.2817[a]	-0.2852[a]	-0.2778[a]	-0.2854[a]	-0.2907[a]	-0.3032[a]
H9	0.2784[a]	0.3562[a]	0.3438[a]	0.3345[a]	0.3482[a]	0.3353[a]	0.3523[a]
O10	-0.2824	-0.2801	-0.2809	-0.2823	-0.2919	-0.2968	-0.2931
C11	0.2409	0.2368	0.2336	0.2336	0.2317	0.2349	0.2419
C12	-0.3063[a]	-0.1755[a]	-0.2217[a]	-0.2246[a]	-0.1849[a]	-0.1702[a]	-0.1874[a]
H13	0.2418[a]	0.3343[a]	0.3923[a]	0.3953[a]	0.3101[a]	0.3048[a]	0.3345[a]
C14	0.2409	0.2324	0.2352	0.234	0.2348	0.2343	0.228
O15	-0.2824	-0.2515	-0.2548	-0.2611	-0.2582	-0.2784	-0.2602
C16	-0.1712	-0.1802	-0.1791	-0.1787	-0.1799	-0.1788	-0.2097
H17	0.2309	0.2392	0.2391	0.2372	0.2415	0.2467	0.3012[a]
C18	-0.2601	-0.2503	-0.2509	-0.2533	-0.2494	-0.2455	-0.269
H19	0.2761	0.286	0.2856	0.2835	0.2865	0.2877	0.2765
C20	-0.3063[a]	-0.1888[a]	-0.1898[a]	-0.1983[a]	-0.1767[a]	-0.1707[a]	-0.2047[a]
H21	0.2418	0.2473	0.2479	0.2448	0.2509	0.2546	0.3028
C22	-0.1712	-0.1835	-0.1914	-0.1908	-0.1793	-0.1807	-0.1927
H23	0.2309	0.2462	0.246	0.2421	0.2398	0.2923[a]	0.2426
C24	-0.2601	-0.2494	-0.2521	-0.2529	-0.2278	-0.2525	-0.2543
H25	0.2761	0.2831	0.2812	0.2803	0.3178	0.2993	0.2802
C26	0.2294	0.2163	0.2166	0.2151	0.2165	0.2322	0.2081
C27	-0.169	-0.1701	-0.1702	-0.17	-0.1705	-0.1741	-0.1681
H28	0.2177	0.2203	0.2202	0.2222	0.2221	0.2229	0.218
H29	0.2177	0.223	0.2228	0.2191	0.2204	0.2213	0.2194
C30	0.2294	0.2182	0.2164	0.2157	0.2212	0.2134	0.2258
C31	-0.169	-0.1712	-0.1708	-0.1707	-0.1636	-0.1992	-0.1855
H32	0.2177	0.2206	0.2206	0.2196	0.2018	0.2124	0.2135
H33	0.2177	0.2196	0.2183	0.2185	0.2452	0.2769[a]	0.2721[a]
C34	-0.6242	-0.6223	-0.6227	-0.6229	-0.6371	-0.6302	-0.6341
H35	0.2151	0.2175	0.2175	0.2171	0.1984	0.195	0.2106
H36	0.1994	0.2022	0.2013	0.2011	0.1862	0.2198	0.2042
H37	0.2151	0.2161	0.2155	0.2157	0.2581	0.2403	0.2128
C38	-0.6242	-0.6242	-0.6241	-0.6243	-0.6234	-0.6207	-0.6272
H39	0.2151	0.2135	0.2138	0.2159	0.2161	0.2181	0.2113
H40	0.1994	0.2023	0.2023	0.2015	0.2026	0.2054	0.1995
H41	0.2151	0.2156	0.2157	0.2137	0.2147	0.2169	0.2127
O42	-	-0.3503	-0.3754	-0.3829	-0.3175	-0.3258	-0.3508
N43	-	0.2182	0.2321	0.2308	0.2129	0.2378	0.2105
O44	-	-0.2479	-0.239	-0.2316	-0.2655	-0.3006	-0.2579
O45	-	-0.3333	-0.3025	-0.325	-0.3447	-0.3145	-0.3374

[a]Atomic charge densities of the most significant variations

calculated using the same level of theory. The optimized molecular geometry of complex **4** and one asymmetric unit of complex **5** are given in Fig. 3. In the case of complex **4**, the interaction between two $[Ag(Etnic)_2NO_3]$ units does not change the molecular geometry around the metal ion. The Ag–O distances are calculated to be in the range of 2.491–

2.625 Å, indicating a more or less distorted tetrahedral geometry around the silver ion. The calculated C–H···O bonding distances are calculated to be weaker than in complex **1**.

On other hand, the packing of four $[Ag(Etnic)_2NO_3]$ complex units changes the situation. Complex **5** has two asymmetric $[Ag(Etnic)_2NO_3]$ complex units differing in the bonding mode of the nitrate group. In one unit, the nitrate group acts as bidentate ligand through two O-atoms while in the second unit the nitrate group acts as monodentate ligand through one oxygen atom (Fig. 3, Table 1). As a result, the molecular geometry around the Ag^+ ion is predicted to be distorted tetrahedral for the former and trigonal planar for the latter. This different behavior of the bonding situation of the nitrate group is dependent on the degree of C–H···O interaction within the molecular units. It was found that the bidentate nitrate forms weaker intramolecular C–H···O interactions compared to the unidentate nitrate ligand (Fig. 3, Table 1). One could predict that, as the degree of C–H···O interaction increases as the Ag···O distances become much longer, the molecular geometry around Ag^+-ion is shifted to trigonal planar rather than tetrahedral. The present calculations predict centroid–centroid distances of 4.82–4.88 Å and offset angles in the range of 15.68–18.37°. These results indicate that the π–π stacking interactions are very weak [46] and have only a negligible effect on the molecular geometry around the Ag^+-ion.

Atomic charge population analysis

The calculated Mülliken atomic charges (MAC) for the studied complexes **1**–**5** using B3LYP/LANL2DZ method are collected in Table 3 where the atomic charge densities of the most significant variations are indicated. The magnitude of the charges at the different atomic sites of the coordinated Etnic ligands is almost the same as in the free Etnic except at the ring nitrogen and at the sites involved in H-bonding interactions (Table 3). The calculated MAC at the N-sites can be seen to increase due to coordination of the Ag^+ ion through the ring nitrogen atom, which induces a charge in the adjacent carbon atoms to more negative (see atomic charges at N2, N4, C6 and C20; Table 3). Furthermore, the formation of C–H···O hydrogen bonds in the studied complexes tends to increase the charge densities at the H-sites involved in such interactions where the formation of the shorter intermolecular C–H···O interaction between $[Ag(Etnic)_2NO_3]$ complex and water molecules increases the charge density at the H-sites more effectively than the longer intramolecular C–H···O interactions (see atomic charges at H13 compared to H9).

The molecular electrostatic potential (MEP) is best suited for identifying the effect of the intra- and intermolecular interactions on the different atomic sites [22]. Figure 4 shows the MEP of Etnic compared to the studied complexes **1**–**5**. The red regions of MEP are related to negative sites while the blue ones are related to positive sites. It can be seen from Fig. 4 that coordination to the metal ion as well as the C–H···O interactions change the electrostatic potential at the N and H-sites involved in such interactions, respectively.

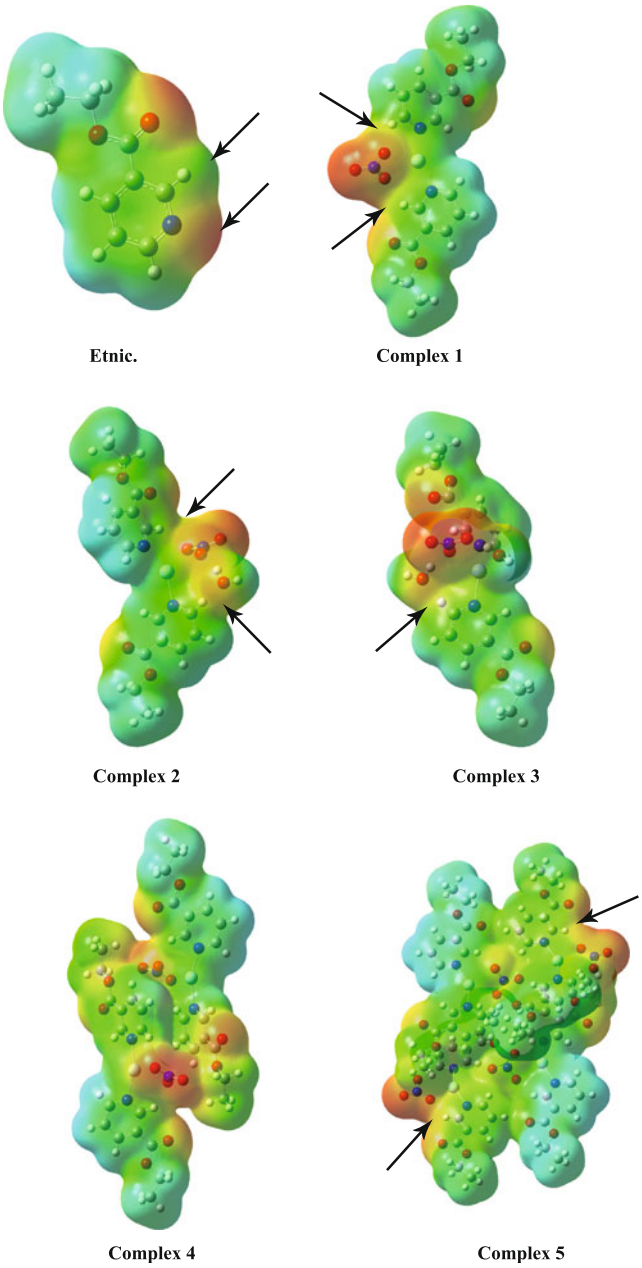

Fig. 4 Molecular electrostatic potentials (MEPs) mapped on the electron density surface calculated by DFT/B3LYP method for studied compounds. Note the variations of the potential at the coordinated nitrogen atom and the H-sites involved in the H-bonding interactions compared to the free Etnic ligand

Conclusions

In this work the molecular structure of the complexes [Ag(Etnic)$_2$NO$_3$]; **1,** [Ag(Etnic)$_2$NO$_3$]$\cdots$H$_2$O; **2,** [Ag(Etnic)$_2$NO$_3$]$\cdots$2H$_2$O; **3,** the dimer [Ag(Etnic)$_2$NO$_3$]$_2$; **4** and the tetramer [Ag(Etnic)$_2$NO$_3$]$_4$; **5** were calculated using the DFT/B3LYP method. The results were compared to model the effect of hydrogen bonding interactions and molecular packing on the molecular structure of the [Ag(Etnic)$_2$NO$_3$] complex. The accurate H-bond dissociation energies of complexes **2** and **3** were calculated using the counterpoise method to be in the range of 12.220–14.253 and 30.106–31.055 kcalmol^{-1}, respectively indicating the formation of moderate to strong H-bonds between complex **1** and water molecules. The hydrogen bonding interactions tends to weaken the Ag-O(NO$_2$) bond. The calculations predict bidentate nitrate ligand in case of **1**, **2** and **4**, leading to more or less distorted tetrahedral molecular geometry around the silver ion. For complex **3**, the nitrate group acts as an unidentate ligand, so distorted trigonal planar geometry around the silver ion is predicted. In the case of complex **5**, there are two asymmetric units of [Ag(Etnic)$_2$NO$_3$] molecules where distorted tetrahedral and trigonal planar geometry are predicted around the silver ion. The calculations predicted almost no change in the charge densities at the different atomic sites except at the atomic sites involved in the C–H$\cdots$O interactions and at the coordinated nitrogen of the pyridine ring.

References

1. Latosinska Jolanta N, Seliger J, Zagar V, Burchardt Dorota V (2012) A comparative study of the hydrogen-bonding patterns and prototropism in solid 2-thiocytosine (potential antileukemic agent) and cytosine, as studied by 1H-14N NQDR and QTAIM/DFT. J Mol Model 18:11–26
2. Nishi K, Matsumoto N, Iijima S, Halcrow MA, Sunatsuki Y, Kojima M (2011) A hydrogen bond motif giving a variety of supramolecular assembly structures and spin-crossover behaviors. Inorg Chem 50:11303–11305
3. Vallejos MA, Angelina EL, Peruchena NM (2010) Bifunctional hydrogen bonds in monohydrated cycloether complexes. J Phys Chem A 114:2855–2863
4. Oliveira BG, Araujo RCMU, Carvalho AB, Ramos MN (2009) The molecular properties of heterocyclic and homocyclic hydrogen-bonded complexes evaluated by DFT calculations and AIM densities. J Mol Model 15:123–131
5. Watson JD, Crick FHC (1953) A structure for deoxyribose nucleic acid. Nature 171:737–738
6. Djokic S (2008) Treatment of various surfaces with silver and its compounds for topical wound dressings, catheter and other biomedical applications. ECS Trans 11(21):1–12
7. Stillman MJ, Presta A, Gui Z, Jiang DT (1994) Spectroscopic studies of copper, silver and gold-metallothioneins. Metal-Based Drugs 1(5–6):375–394
8. Guo Z, Sadler PJ (1999) Metals in medicine. Angew Chem Int Ed 38:1512–1531
9. Ahmad S, Isab AA, Ali S, Al-Arfaj AR (2006) Perspectives in bioinorganic chemistry of some metal based therapeutic agents. Polyhedron 25:1633–1645
10. Legler AV, Kazachenko AS, Kazabanov VL, Peryanova OV, Veselova OF (2001) Synthesis and antimicrobial activity of silver complexes with arginine and glutamic acid. Pharm Chem J 35:501–503
11. Chernyavskaya AA, Loginova NV, Polozov GI, Shadyro OI, Sheryakov AA, Bondarenko EV (2006) Synthesis and antibacterial activity of silver (I) and copper (II) complexes with 2-(4,6-Di-tert-butyl-2,3-dihydroxyphenylsulfanyl)acetic acid. Pharm Chem J 40:413–415
12. Criado JJ, Rodriguez-Fernandez E, Garsia E, Hermosa MR, Monte E (1998) Thiourea derivatives of α-aminoacids. Synthesis and characterization of Ni(II), Cu(II) and Pt(II) complexes with l-valinate derivatives. Antifungal activity. J Inorg Biochem 69:113–119
13. Kazachenko AS, Legler AV, PerYanova OV, Vstavskaya Y (2000) Synthesis and antibacterial activity of silver complexes with histidine and tryptophan. Pharm Chem J 34:257–258
14. Ali MA, Mirza AN, Hossan M (2001) Synthesis, characterization, antifungal properties and X-ray crystal structures of five- and six-coordinate copper(II) complexes of the 6-methyl-2-formylpyridine^{4}N-dimethylthiosemicarbazone. Polyhedron 20:1045–1052
15. McCann M, Coyle B, Briody J, Bass F, O'Gorman N, Devereux M, Kavanagh K, McKee V (2003) Synthesis and antimicrobial activity of (Z)-3-(1*H*-imidazol-1-yl)-2-phenylpropenenitrile and its metal complexes: X-ray crystal structures of the Zn(II) and Ag(I) complexes. Polyhedron 22:1595–1601
16. Li Q, Tang H, Li Y, Wang M, Wang LF, Xia CG (2000) Synthesis, characterization, and antibacterial activity of novel Mn(II), Co(II), Ni(II), Cu(II), and Zn(II) complexes with vitamin K$_3$-thiosemicarbazone. J Inorg Biochem 78:167–174
17. Abu-Youssef MAM, Langer V, Öhrström L (2006) A unique example of a high symmetry three- and four-connected hydrogen bonded 3D-network. Chem Commun 1082–1084
18. Abu-Youssef MAM, Langer V, Öhrström L (2006) Synthesis, a case of isostructural packing, and antimicrobial activity of silver (I)quinoxaline nitrate, silver(I)(2,5-dimethylpyrazine) nitrate and two related silver aminopyridine compounds. Dalton Trans 2542–2550
19. Abu-Youssef MAM, Dey R, Gohar Y, Massoud AA, Öhrström L, Langer V (2007) Synthesis and structure of silver complexes with nicotinate-type ligands having antibacterial activities against clinically isolated antibiotic resistant pathogens. Inorg Chem 46:5893–5903
20. Massoud AA, Langer V, Abu-Youssef MAM (2009) Bis[4-(dimethylamino)pyridine-κN^1]-silver(I) nitrate dehydrate. Acta Crystallogr C65:352–354
21. Abu-Youssef MAM, Soliman SM, Langer V, Gohar YM, Hasanen AA, Makhyoun MA, Zaky AH, Öhrström LR (2010) Synthesis, crystal structure, quantum chemical calculations, DNA interactions, and antimicrobial activity of [Ag(2-amino-3-methylpyridine)$_2$]NO$_3$ and [Ag(pyridine-2-carboxaldoxime)NO$_3$]. Inorg Chem 49:9788–9799
22. Soliman SM (2012) Molecular structure and vibrational spectra of free and coordinated 3-bromoquinoline: unexpected intramolecular C–H$\cdots$O interactions. J Mol Struct 1017:135–142
23. Chen CL, Kang BS, Su CY (2006) Recent advances in supramolecular design and assembly of silver(i) coordination polymers. Aust J Chem 59:3–18
24. Khlobystov AN, Blake AJ, Champness NR, Lemenovskii DA, Majouga AG, Zyk NV, Schroder M (2001) Supramolecular design of one-dimensional coordination polymers based on silver(I) complexes of aromatic nitrogen-donor ligands. Coord Chem Rev 222:155–192

25. Takeshima T, Takeushi H, Eguawa T, Konaka S (2003) Gas-phase molecular structure of nicotinamide studied by electron diffraction combined with MP2 calculations. J Mol Struct 644:197–205
26. Velcheva EA, Daskalova LI (2005) The experimental and computational study on the IR spectra and structure of pyridine-3-carboxamide (nicotinamide)-d_0 and -d_2. J Mol Struct 741:85–92
27. Fu A, Du D, Zhou Z (2003) Density functional theory study of vibrational spectra of acridine and phenazine. Spectrochim Acta Part A 59:245–253
28. Handy NC, Maslen PE, Amos RD, Andrass JS, Murrey CW, Laming G (1992) The harmonic frequencies of benzene. J Chem Phys Let 506–515
29. Bakiler M, Bolukbasi O, Yilmaz A (2007) An experimental and theoretical study of vibrational spectra of picolinamide, nicotinamide, and isonicotinamide. J Mol Struct 826:6–16
30. Ramalingam S, Periandy S, Govindarajan M, Mohand S (2010) FT-IR and FT-Raman vibrational spectra and molecular structure investigation of nicotinamide: a combined experimental and theoretical study. Spectrochim Acta Part A 75:1552–1558
31. Dimitrov Y, Daskalova LI (2009) Theoretical study of the vibrational spectra of the hydrogen-bonded systems between pyridine-3-carboxamide (nicotinamide) and DMSO. Spectrochim Acta A Mol Biomol Spectrosc 71:1720–1727
32. Zhengyu Z, Dongmei D, Khan SUM (2000) Calculation of the energy of activation in the electron transfer reaction not involving the bond rupture at the electrode. J Mol Struct (THEOCHEM) 505:247–255
33. Zhengyu Z, Aiping F, Dongmei D (2000) Studies on density functional theory for the electron-transfer reaction mechanism between M–C_6H_6 and M^+–C_6H_6 complexes in the gas phase. Int J Quant Chem 78:186–194
34. Kumar M, Jaiswal S, Singh R, Srivastav G, Singh P, Yadav TN, Yadav RA (2010) Ab initio studies of molecular structures, conformers and vibrational spectra of heterocyclic organics: I. Nicotinamide and its N-oxide. Spectrochim Acta A 75:281–292
35. Arıcı K, Yurdakul M, Yurdakul S (2005) HF and DFT studies of the structure and vibrational spectra of 8-hydroxyquinoline and its mercury(II) halide complexes. Spectrochim Acta A 61:37–43
36. Lakshmi A, Balachandran V, Janaki A (2011) HOMO–LUMO and NBO analysis of 5,7-dibromo-8-hydroxyquinoline and 5,7-dichloro-8-hydroxyquinoline based on Density Functional Theory. J Mol Struct 1004:51–66
37. Dziembowska T, Szafran M, Jagodzin'ska E, Natkaniec I, Pawlukojc' A, Kwiatkowski JS, Baran (2003) DFT studies of the structure and vibrational spectra of 8-hydroxyquinoline N-oxide. Spectrochim Acta A 59:2175–2189
38. Ozel AE, Kecel S, Akyuz S (2006) Molecular structure and vibrational assignment of 2-,4-,6-methylquinoline by density functional theory (DFT) and ab initio Hartree-Fock (HF) calculations. Vib Spectrosc 42:325–332
39. Sundaraganesan N, Kalaichelvan S, Meganathan C, Dominic Joshua B, Cornard J (2008) FT-IR, FT-Raman spectra and ab initio HF and DFT calculations of 4-N, N -dimethylamino pyridine. Spectrochim Acta A 71:898–906
40. Ramalingam S, Periandy S, Govindarajan M, Mohan S (2010) FT-IR and FT-Raman vibrational spectra and molecular structure investigation of nicotinamide: a combined experimental and theoretical study. Spectrochim Acta A 75:1552–1558
41. http://www.ccdc.cam.ac.uk/data_request/cif
42. Frisch MJ et al (2004) Gaussian 03, Revision C.01. Gaussian, Wallingford
43. Schuchardt KL, Didier BT, Elsethagen T, Sun L, Gurumoorthi V, Chase J, Li J, Windus TL (2007) A community database for computational sciences. J Chem Inf Model 47:1045–1052
44. Zhao Y, Truhlar DG (2005) Benchmark databases for nonbonded interactions and their use to test density functional theory. J Chem Theor Comput 1(3):415–432
45. Dennington R II, Keith T, Millam J (2007) GaussView, Version 4.1. Semichem, Shawnee Mission
46. Janiak C (2000) A critical account on π-π stacking in metal complexes with aromatic nitrogen-containing ligands. J Chem Soc Dalton Trans 3885–3896